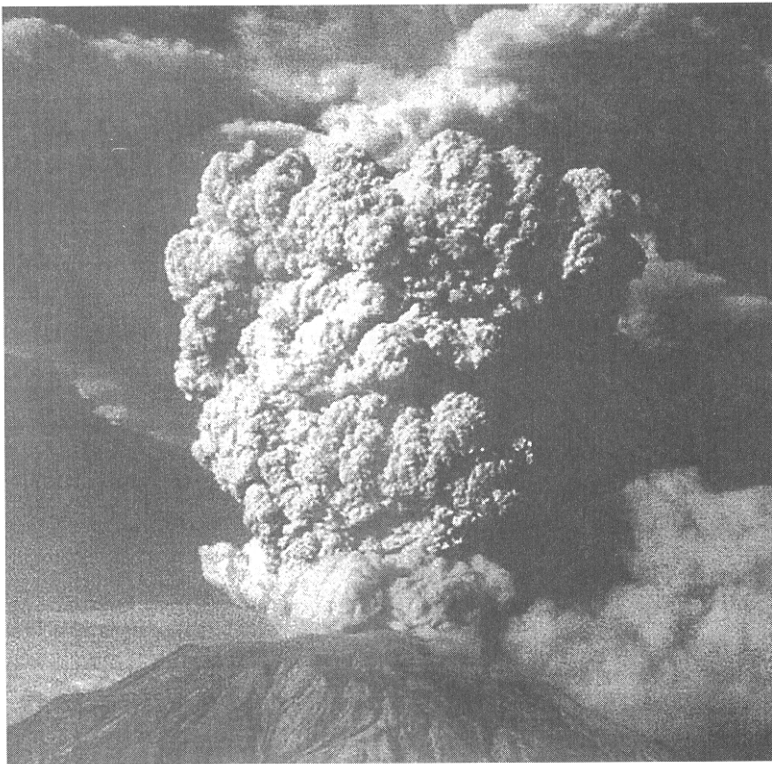


## Geometry of homogeneous scalar turbulence: iso-surface fractal dimensions $5/2$ and $8/3$

•*Illustrated chapter foreword.* The photograph below, taken by M.P. Doukas and reprinted courtesy of the United States Geophysical Survey, is discussed on the next page.



An exception in this book, the preceding page reproduces an actual photograph of a natural event: Mt. St. Helens after its top blew off. In vulcanology, the practical challenge is to predict eruptions and the dream, to control them. The scientific challenge is to explain every quantitative observation and reduce all scientific and practical predictions to the status of corollaries. While all those worthy challenges continue to be pursued, an intermediate pragmatic challenge is to describe what is observed and perhaps achieve at least a taxonomy of volcanic events.

An eye attuned to fractals recognizes in the preceding page a collection of billows upon billows upon billows – a textbook example of fractality. About those whose eye is innocent of fractals, one may wonder who organizes the evidence better, the “layman” or the typical quantitative scientist, namely, a person selected and exclusively trained on the basis of skills in algebra and analysis?

During the centuries before photography, Italy left an abundant pictorial representation of volcanoes that can be sampled in Scarth 1999. Few great artists were involved and the early pictures look crude and some look unrealistic and/or atypical. But one of Scarth's figures subdivides every billow of every “billowing” level into 2 by 2 smaller ones.

The result presents an uncanny kinship to a cartoon of reality constrained to an almost regular 2 by 2 grid. The painter's eye, brain and hand contribute to each picture in ways one cannot separate. It is rather fascinating to find that a journeyman painter of long ago simplified actual billowing by recursive interpolations, in the same way as twentieth century high mathematicians.

The representations of volcanoes impact a very important theme which this book often mentions but cannot develop. Following my teachers, I used to believe and repeat that fractals were “invented” circa 1900 as mathematical monsters. Had this notion been historically correct, it would have been hard to understand how the practically non-existent popular response to the monsters changed over a few years to a highly positive popular response to fractal geometry.

In fact, the notion that fractals are a hundred years old and were invented by mathematicians is emphatically disproved by history, as sketched in Section 1.5 of Chapter H8. One should now view fractals as dating back to the dawn of humanity and having moved from art back to art, through mathematics, finance, and a multitude of sciences. Now, every properly alerted person recognizes many unmistakable traces of informal fractality everywhere – for example in old paintings of volcanoes.

Be that as it may, awareness of fractals used to be wholly informal and haphazard, but today the eye can be trained so that the Mt. St. Helens picture evokes fractality without question or delay. •

♦ **Abstract.** This paper studies several geometric aspects of Poisson and Gaussian random fields that approximate Burgers  $k^{-2}$  fields and Kolmogorov  $k^{-5/3}$  homogeneous turbulence. Model scalar iso-surfaces (e.g., of constant temperature or concentration) are illustrated, and their relative degrees of wiggleness are shown to be characterized best by fractal dimensions equal to  $3 - 1/2$  (Burgers) and  $3 - 1/3$  (Kolmogorov). ♦

TURBULENCE IN FLUIDS RAISES A VARIETY OF PROBLEMS of geometry. They are important but so far have not received the full attention they deserve.

## 1. INTRODUCTION

The theory of stochastic processes (greatly influenced – through N. Wiener – by Perrin's work on Brownian motion and G. I. Taylor's early papers on turbulence) grasped fully the peculiar and “pathological” shapes of randomly generated lines and has either borrowed or developed analytic and geometric tools to describe this kind of irregularity. But geometry (in contrast to analysis) has hardly been applied to the specific random surfaces of turbulence. This failure is particularly surprising because turbulent shapes are readily visualized and, therefore, almost cry out for a proper geometrical description.

The present paper is one in a series that I am devoting to this goal. M 1972j{N14} and M 1974f{N15} dealt with intermittency. The present work, which can be read independently, returns to a more traditional context and investigates certain geometric aspects of the random fields of the classic theory of homogeneous turbulence (Kolmogorov). More precisely, we shall study two approximations. The more familiar approximation is the zero-mean random Gaussian field, for which the variance of the increments obeys the  $2/3$  law. The less familiar approximation, to be called a Poisson field, can be viewed also as a (new) algorithm designed to simulate the above Gaussian field on a computer. The elementary steps of this

algorithm may seem to have a possible concrete interpretation in terms of “shocks” but are in fact mere mathematical devices.

To give an idea of the geometry, we exhibit actual simulations of the iso-surfaces of scalar quantities, such as the surfaces of constant temperature, and comment on their shapes. We stress the fact that in the case of Gaussian fields the iso-surfaces are convoluted to such an extraordinary extent that it is best to consider them as lying “in-between” ordinary surfaces and solids and, more precisely, as having a dimension equal to  $8/3$ . Similarly, although in this case the proof is as yet incomplete, it appears that the four-dimensional Euclidean graph of the function giving the temperature at a point has a dimension equal to  $11/3$ .

The concept of a fractional (Hausdorff) dimension has been known in pure mathematics for over half a century, a good reference being Rogers 1970. It is particularly potent in describing the fine structure of random functions. However, it remained a little-known curiosity, even among mathematicians. No concrete application was suspected until it was injected systematically into natural science, first through the study of certain noises (M 1965c{N7}), then through the shape of the earth's surface (M 1967s), and ultimately through the study of turbulence (M 1972j{N14}, 1974f{N15}). No presentation directed towards scientists was attempted until recently (M 1975o), and its range of application is far from having been exhausted. For reasons I cannot describe here, the corresponding sets can be called fractals and the term “fractional dimension” is best replaced by “fractal dimension.” Applications of fractals to turbulence are described in M 1976c{N19}, M 1976o{N18} and Scheffer 1975.

For the sake of clarity, the argument will be carried out first for the corresponding Poisson and Gaussian approximations to Burgers homogeneous “turbulence;” this is extremely crude as a model, but it is much simpler and, hence, provides useful insight into reality. The fractal dimension of Burgers iso-surfaces is 2.5.

The discussion includes an application of another concept which was once considered to be a mathematical curiosity. A scalar Burgers Gaussian field, we shall discover, is identical to Lévy's 1948 independently developed concept of a “Brownian function” in space; by analogy, we shall propose for the scalar Kolmogorov Gaussian field the term “fractional Brownian function.”

## 2. THE GEOMETRY OF RANDOM SCALAR FIELDS WITH BURGERS VARIANCE AND POISSON AND GAUSSIAN DISTRIBUTIONS, THAT IS, BROWNIAN FUNCTIONS OF A POINT

In the one-dimensional Burgers model, turbulence has a spectral density proportional to  $k^{-2}$ . At least since von Neumann 1963, it has been customary to apply the term "Burgers turbulence" to a collection of step-like discontinuities in three dimensions. We shall first study a scalar turbulence field, such as the temperature  $B(P)$  at the point  $P$  or the concentration of an inert contaminant (see Corrsin 1951). For two points  $P'$  and  $P''$  in a Burgers scalar field,  $\langle [B(P') - B(P'')] ] \rangle = 0$  and  $\langle [B(P') - B(P'')] ]^2 \rangle = |\overline{P'P''}|$ .

### 2.1. Poisson fields

A precise mathematical model of a Burgers field is the Poisson field. This field results from an infinite collection of "steps" (for example, of temperature) whose directions, locations and intensities are given by three infinite sequences of mutually independent random variables. The locations can be determined by the distances from the planes carrying the steps to the origin  $O$ . These distances must form a Poisson sequence of positive numbers  $R_n$ . By definition, a Poisson sequence of inverse density  $\mu$  is such that the probability of finding at least one point between  $R \geq 0$  and  $R + dR \geq 0$  is  $dR/\mu$ . The directions of these planes can be determined by the altitudes drawn to them from  $O$ , and must be given by a sequence of points  $H_n$  on the unit sphere on which the probability of finding a point  $H_n$  in any domain of area  $dS$  is  $dS/4\pi$ . Finally, the amplitudes can be represented by a sequence of random quantities  $Q_n$  that are arbitrary except that they have a symmetric distribution and a finite variance  $\langle Q_n^2 \rangle$ , which will be assumed to be normalized to unity.

Because  $\langle Q_n^2 \rangle = 1$ ,  $\langle Q_n \rangle$  is necessarily finite and because the distribution is symmetric, the quantity  $\langle Q_n \rangle$  must vanish. Thus to each  $n$  there will correspond a point  $V_n$ , a plane  $\Pi_n$  and a function  $D_n$ . The point  $V_n$  is such that  $\overline{OV_n}R_n = \overline{OH_n}$ , that is, the plane is perpendicular to  $\overline{OV_n}$  through  $V_n$ . The plane is the locus of all points  $P$  such that  $\overline{OP} \cdot \overline{OH_n} = R_n$ . Finally, the function  $D_n F(P)$  vanishes where  $\overline{OP} \cdot \overline{OH_n} < R_n$  (in particular, at the point  $O$ ); this function equals  $Q_n$  when  $\overline{OP} \cdot \overline{OH_n} > R_n$  and equals  $Q_n/2$  when  $\overline{OP} \cdot \overline{OH_n} = R_n$ . Because of this last property and the symmetry of the distribution of  $Q$ , the distribution of  $D_n F(P)$  is isotropic. Note also that, even if  $Q$  is Gaussian, the joint distribution of two or more values of  $D_n F(P)$  is not Gaussian; hence,  $D_n F(P)$  is never a Gaussian field. Adding all the contributions  $D_n F(P)$ , one defines a Poisson field as

$$F(P) = \sum_{n=1}^{\infty} D_n F(P).$$

The above construction involves a specific origin  $O$ , but it is easy to see that the distribution of the planes of discontinuity remains invariant as  $O$  is displaced. Therefore, the field  $F(P)$  is also invariant, in the sense that the distribution of  $F(P') - F(P'')$  for any two fixed points  $P'$  and  $P''$  is invariant. In particular, the number of planes of discontinuity intersecting any bounded domain is almost surely finite. When this domain is an arbitrary segment  $\overline{P'P''}$ , the number of intersecting planes is a Poisson random variable of expectation  $\lambda |\overline{P'P''}|$ , with  $\lambda$  proportional to  $\mu$ ; as Burgers wanted,

$$\langle F(P') - F(P'') \rangle = 0 \text{ and } \langle [F(P') - F(P'')]^2 \rangle = \lambda |\overline{P'P''}|.$$

The fact that  $F(P') - F(P'')$  is affected only by “local” planes (defined as those which intersect  $\overline{P'P''}$ ) expresses that this field is local, in one sense at least; but the matter of local versus global properties also has other aspects, to which we shall return in Section 4.

The probability distribution of a scalar Poisson field is not universal but depends on the distribution of  $Q$ . For example, unless  $Q$  itself is Gaussian, the probability distribution of  $F(P) - F(O)$  depends strongly upon the number of contributing terms  $D_n F(P)$  and hence upon the value of  $|\overline{OP}|$ . For large  $|\overline{OP}|$ , the central limit theorem applies, and  $F(P) - F(O)$  tends to a Gaussian distribution irrespective of the distribution of  $Q$ . To the contrary, for small  $|\overline{OP}|$ ,  $F(P)$  may have a variety of shapes.

## 2.2. Brownian fields

Von Neumann 1963 (p. 450) asserts that “It would appear that the Burgers approach describes a fixed number of shocks of fixed size correctly, but it seems questionable whether its conclusions still apply to an asymptotically (with time) increasing number of (individually) asymptotically weakening shocks. Yet, this is probably the pattern of hydrodynamical shocks in those cases where they combine with turbulent motion.”

It is not clear which “conclusions” von Neumann had in mind, but the mathematical construction of a field made of such shocks is possible. Indeed, Lévy 1948 defined the scalar Brownian function  $B(P)$  of a point  $P$  as the scalar Gaussian field such that

$$\langle B(P') - B(P'') \rangle = 0 \text{ and } \langle |B(P') - B(P'')|^2 \rangle = |\overline{P'P''}|.$$

This field  $B(P)$  is the (unique) Gaussian interpolate of a Burgers field. In addition, one can relabel the Poisson field defined in Section 2.1 as  $F_\lambda(P)$ , and show that the Burgers field  $B(P)$  is the limit for  $\lambda \rightarrow \infty$  of the infinite sequence of Poisson fields  $\lambda^{-1/2}F_\lambda(P)$ . This limit process implements fully the notion of an increasing number of increasingly weak discontinuities. (The concept of the limit of a random field has many different aspects. In this case, it suffices that, for any set of points  $P_n$ , the probability distribution of the vector with coordinates  $\lambda^{-1/2}F_\lambda(P_n)$  should converge to the probability distribution of the vector with coordinates  $B(P_n)$ .) Conversely, the possibility of defining  $B(P)$  through this limit process eliminates the artificiality (underlined by Lévy) that has characterized earlier methods for generating  $B(P)$ , and it yields a method (not known to Lévy) for performing computer simulations.

A Brownian field is extremely irregular, but this fact cannot be illustrated directly, because we cannot draw four-dimensional graphics. However, such a field's planar or linear sections are well-known and of independent interest. M 1975w{H19} and M 1975O propose the function  $B(x, y, 0)$  as a crude model of the earth's surface and the section along the  $x$ -axis reduces to Wiener's Brownian motion  $B(x, 0, 0)$ . However, even more illustrative of  $B(P)$  is the structure of its iso-sets  $B(P) = \text{constant}$ , as it is fully exemplified by the set  $B(P) = 0$ .

### 2.3. Poisson iso-surfaces

For a continuous function  $G(P)$ , an iso-surface is a set of points where  $G$  assumes the same value. However, this concept does not apply to  $F(P)$ , because it is not continuous. It follows, for example, that the points where  $F(P) = 0$  reduce almost surely to a small volume around  $O$ , bounded by a finite number of planes of discontinuity.

However, one may well choose to extend the definition of the iso-set  $F(P) = 0$  to include all the points which have both a neighborhood where  $F \geq 0$  and a neighborhood where  $F \leq 0$ . If so, the iso-set almost surely includes a surface composed of an infinite number of small bounded pieces of the plane. In addition, it includes the previously mentioned small volume near  $O$ . Alternatively, if the constant  $C$  is chosen at random with a continuous distribution, the iso-set  $F(P) = C$  is simply a surface.

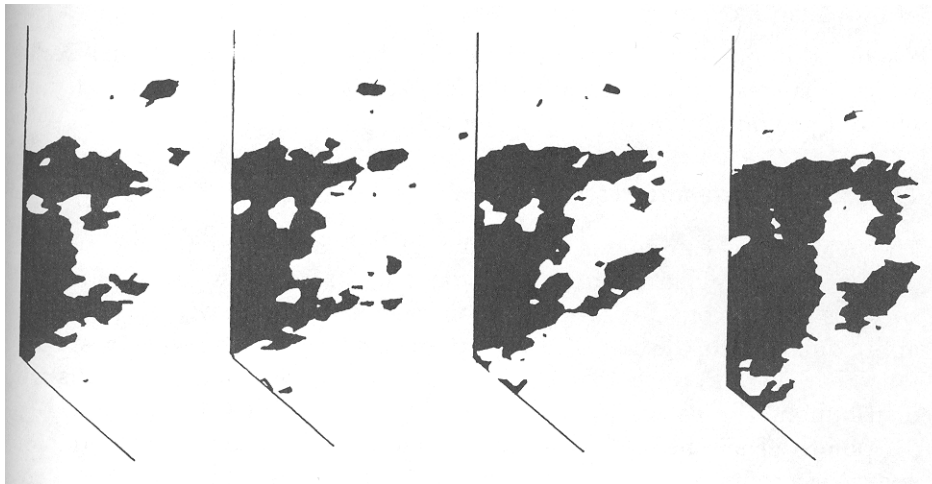


FIGURE C18-1. Four successive slices of a computer-generated approximation to the volume  $B(P) > 0$ , where  $B(P)$  is the Gaussian approximation to a Burgers scalar field at a point  $P$  in space. Clearly, these drawings are much too smooth to represent actual turbulence (see Figure 2), but it has not escaped the author's attention that they are reminiscent of various portions of the earth's surface: Greece, the Sea of Okhotsk (as seen in a mirror), the Gulf of Siam or perhaps Western Scotland. In other publications, the author has shown that, while such a resemblance is in no way unusual, many other parts of the world are smoother and require a fractional Brownian model with a larger value of  $H$  than either the Burgers or the Kolmogorov models of turbulence. Note that, although the black and white regions are identical in their statistical properties, the white one is by far the larger. The above graphs do not include the "empty" portions of the square slices.



## 2.4. Cutoffs

When one takes viscosity into account, the discontinuous functions  $D_n(P)$ , the Poisson field and the limiting Brownian field  $B(P)$  have no physical meaning. Nevertheless, the fine structure of  $B(P)$  is very interesting, and even more interesting is the fine structure of the Gaussian field  $\tilde{B}(P)$  with Kolmogorov variance (see Section 3). We hope, of course, that this fine structure is not due entirely to the use of the Gaussian approximation, but (being unable to tell) we choose not to worry about this. Even in cases where the fine structure corresponds to inaccessible asymptotics, it is useful to know it, because it simplifies and clarifies the fine structures above the cutoff. Such was the opinion of Perrin (whom we shall soon quote on a related matter) concerning the importance of the fine structure of Brownian movement.

In addition, the Brownian field  $B(P)$  has an infinite external scale, which may be physically unrealistic, but is very difficult to change without profoundly modifying the model.

## 2.5. Brownian iso-surfaces

The field  $B(P)$  is continuous so that the set  $B(P) = 0$  is a continuous surface and its statistical structure and shape are characteristic of all the iso-surfaces  $B(P) = \text{constant}$ . Figure 1 shows several successive "slices" of an approximation to the set  $B(P) = 0$ , constructed on the basis of a special Poisson field  $F(P)$  such that  $Q_n$  follows an approximation to a Gaussian distribution. The values of  $B(P)$  were first evaluated over a spatial grid of  $51^3$  points. Then, because no standard computer routine was available for spatial interpolation, smooth interpolates of the lines where  $B(P) = 0$  were drawn separately for each horizontal planar grid of  $51^2$  points. Hence, the smoothness of the line drawn in each of these planes is an artifact. The discontinuities seen between the different planes are also artifacts for the same reason. The main feature of the limit field  $B(P)$  is that it is isotropic and has no intrinsic scale at all. Therefore, the local detail seen on the surfaces  $B(P) = 0$  should be disregarded and replaced by mentally interpolating reduced-scale versions of what we see of the medium-sized and large-detail. The result is extremely (in fact, infinitely) irregular: the biggest visible piece is surrounded by blobs, jetsam and flotsam of all shapes and sizes and by "negative image" versions that are scattered in its interior. In addition, the outside branches out into filaments of every kind penetrating the inside, and conversely.

A special hindrance to intuition is that, since the distribution of  $B(P)$  is symmetric, the zones where  $B(P) > 0$  and  $B(P) < 0$  are statistically identical in their geometric properties. Nevertheless, the notion that a shape can be qualitatively identical to its complement is not as difficult to comprehend as it might seem. This is especially true in the present case. Although the regions  $B > 0$  and  $B < 0$  have identical expected volumes, the volumes actually observed in a sample (more precisely, those of the intercepts of these regions with a large sphere of center  $O$ ) may be quite different.

**Digression.** It is interesting, at this point, to quote an excerpt concerning colloids from the preface of a classic book, Perrin 1913.

“Consider one of the white flakes that are obtained by salting a soap solution. At a distance its contour may appear sharply defined, but as soon as we draw nearer its sharpness disappears. The eye no longer succeeds in drawing a tangent at any point on it; a line that at first sight would seem to be satisfactory, appears on closer scrutiny to be perpendicular or oblique to the contour. The use of a magnifying glass or microscope leaves us just as uncertain, for every time we increase the magnification we find fresh irregularities appearing, and we never succeed in getting a sharp, smooth impression, such as that given, for example, by a steel ball.”

A very reasonable implementation of what Perrin had in mind seems to be provided by the surface  $B(P) = 0$ . The surface  $\tilde{B}(P) = 0$  of Section 4 might be even better. Furthermore, the analogy may well go beyond mere geometry; it may be that (a) Perrin's flakes fill the zones where some threshold of concentration of soap is exceeded, and that (b) the said concentration is a manifestation of very mature turbulence.

## 2.6. Rectilinear cross-sections of the Poisson and Brown iso-surfaces

First, the plane cross-section of  $B(P) = 0$  is an iso-line of  $B(x, y, 0) = 0$ . Thus, it is an ocean-level line of a crude image of the earth's surface, that is, it is a crude image of an ocean coastline (M 1967s, 1975w{H19}). Next, the rectilinear cross-section of  $B(P) = 0$  is the set of zeros of ordinary Brownian motion. Similarly, the rectilinear cross-section of  $F(P) = 0$  in a Poisson field is the set of zeros of a Poisson process. Both sets barely differ from the zeros of a random walk. For an example, the reader is referred to Feller 1950 (Vol. 3rd edition), which includes an illustration (Chap. III, Figure 4) and a discussion (Section III.6). The zeros' most striking feature lies in their strongly hierarchical nature: they come in clusters, which combine into super clusters, then in turn into super-super-clusters, and so forth, ad

infinitum. As one views the whole ever more closely, fine detail that seemed like a smooth piece of surface gradually decomposes into many separate folds; correspondingly, what seemed like an isolated intersection of a smooth surface and a line decomposes into many distinct points. As one comes closer to any of the folds, the same process repeats again and again. In the case of a Poisson field, the process is finite, but in the case of a Brownian field, it is endless; increasingly finer folds are continually revealed. Finally, in a Poisson or Brownian field that has been smoothed to take viscosity into account, a finite number of steps leads to a surface that has neither flat portions nor bends.

## 2.7. The Burgers iso-set $B(P) = 0$ is fractal and its dimension is 2.5

Our intuitive feeling for geometric shape has been developed by the study of patterns that are enormously simpler than the ones we are now investigating, such as threads and veils or, to use the terminology of Kuo & Corrsin 1972, "blobs, rods, slabs and ribbons." We therefore experience great difficulty in comprehending and labelling patterns that are extremely irregular. For example, the set  $B(P) = 0$  is, intuitively, more "space-filling" than an ordinary surface or veil but of course is less "space-filling" than an ordinary solid. Let us now demonstrate that the loose notion of unequal degrees of filling can be made more rigorous, and at the same time can be strengthened, by showing that it can be measured by a single number  $D < 3$ , to be called a "fractal" (sometimes "fractional") dimension. This concept (as we have already stated) has been featured in several papers concerning the intermittency of turbulence, but the results obtained in those papers are not required in order to follow the present argument. I even believe that acceptance of the concept of  $D$  will be promoted if the present discussion abstains from referring to earlier applications. Also, to minimize the technical difficulty, we shall adopt an approach that is somewhat unusual and admittedly controversial. Among many near-identical definitions of  $D$ , we shall pick one that is both intuitive and conducive to a very direct proof.

Let us select in an "appropriate fashion" (see below) a large, test cube in space, whose side  $L$  will be the external scale. Then subdivide it into  $(L/\eta)^3$  small cells, whose side  $\eta$  will be the internal scale. Finally, count the number  $N(L, \eta)$  of cells that include at least one point where  $B(P) = 0$ . When one proceeds in this fashion with an ordinary curve – that is, a curve having a well-defined length – it can happen that the curve and the test cube do not intersect, in which case  $N(L, \eta) = 0$ ; such cases are without interest. In other words, the appropriate test cubes are those which actu-

ally intersect the object being tested, and for them one finds that  $N(L, \eta)$  is about  $L/\eta$  (the meaning of “is about” need not be discussed here). Similarly, if a test cube is chosen such that it intersects an ordinary surface,  $N(L, \eta)$  is about  $(L/\eta)^2$ . Finally, with an ordinary solid, the appropriate  $N(L, \eta)$  is about  $(L/\eta)^3$ . The exponents are the Euclidean dimensions.

However, with the pattern of points  $B(P)=0$ , we shall prove in a moment that  $\langle N(L, \eta) \rangle = (L/\eta)^{2.5}$ ; thus, by analogy with the above role of the Euclidean dimension, one may call  $D=2.5$  the dimension of our pattern. It falls below 3 by an amount equal to  $H$ , where the variance of  $B(P') - B(P'')$  is  $|P'P''|^{2H}$ . Let us mention in advance that in the Kolmogorov model, to be discussed in Section 3, the corresponding dimension will follow the same general rule; hence, it will be found to be equal to  $D=8/9=3-1/3$ . The amount by which this value exceeds 2 is greater than that amount for the present  $D=2.5$ , and indeed the pattern is more extremely convoluted.

Return to the field  $B(P)$ . In four-dimensional Euclidean space, Yoder 1974 (first part of the theorem in the appendix) showed that  $D=3.5$  for the set of points  $[x, y, z, B(x, y, z)]$ . Thus, here (in all non-pathological cases of which the author is aware) the fractal dimension exhibits the same behavior under intersection as a Euclidean dimension: it exceeds the dimension of the iso-sets by one.

## 2.8. Proof that the set $B(P)=0$ has a well-defined fractal dimension $D$

In this subsection we shall prove that there exists a constant  $D$  such that  $\langle N(L, \eta) \rangle \sim (L/\eta)^D$ . This argument will remain valid in Section 3. In the next subsection we shall prove that in the Burger's case  $D=2.5$ .

For the first part, we take a non empty cube, and write  $\langle N(L/\eta) \rangle$  as the product of two terms: the total number of cells  $(L/\eta)^3$ , and the conditional probability  $f(L, \eta)$  of a cell being non empty. The probability  $f(L, \eta)$  is obviously a function of  $L/\eta$  because of the self-similarity (scalelessness) of the overall definitions. Let us show that it must in fact be of the form  $(L/\eta)^{D-3}$ . Pick two ratios  $r_1$  and  $r_2$ , and consider a cell of side  $\eta_1 = r_1 L$  and a subcell in it of side  $\eta_2 = r_1 r_2 L$ . One has:

$$\begin{aligned} & \text{Pr \{subcell being non-empty if one knows that the cube is non-empty\}} \\ &= \text{Pr \{subcell being non-empty if one knows that the cell is non-empty\}} \\ &\times \text{Pr \{cell being non-empty if one knows that the cell is non-empty\}}. \end{aligned}$$

Hence,

$$f(L, r_1 r_2 L) = f(r_1 L, r_1 r_2 L) f(L, r_1 L).$$

By iteration,

$$f(L, r^n L) = [f(L, rL)]^n.$$

Since  $r^n L = \eta$ , this yields

$$\log f(L, \eta) = n \log f(L, rL) = \log (L/\eta) \log f(L, rL) / \log (1/r).$$

Denoting  $\log f(L, rL) / \log (1/r)$  by  $3-D$ , we prove that  $f(L, \eta) = (L/\eta)^{3-D}$  for certain  $L$  and  $\eta$ ; the desired result follows by a well-known interpolatory argument.

## 2.9. Outline of a proof that $D = 2.5$ in the Burgers case

Consider a vertical stack of cells of side  $\eta$  within the large cube, and designate by  $N_1(L, \eta)$  the number of those cells which intersect  $B(P) = 0$ . It is not hard to believe, and we shall assert it without proof, that the conditional probability distribution of this number, knowing that  $N(L, \eta) > 0$ , is the same for every stack; the same is true of its probability of being non zero. Since there are  $(L/\eta)^2$  such stacks, we see that  $\langle N(L, \eta) \rangle = (L/\eta)^2 \langle N_1(L, \eta) \rangle$ . Therefore, the result we wish to prove now takes the form  $\langle N_1(L, \eta) \rangle \sim (L/\eta)^{0.5}$ . Next, replace  $N_1(L, \eta)$  by a variant defined as follows. First, draw a "central line" through the centers of all the cells of side  $\eta$  in our stack, where this central line consists of  $L/\eta$  segments of length  $\eta$ . Second, count the number  $\tilde{N}_1(L, \eta)$  of cells that contain at least one point where  $B(P) = 0$ . The function  $B(P)$  being continuous, we can safely believe that  $\langle N_1(L, \eta) \rangle$  differs from  $\langle \tilde{N}_1(L, \eta) \rangle$  only by a random factor of the order of unity, independently of  $L$  and  $\eta$ .

Moreover, one can write  $\langle \tilde{N}_1(L, \eta) \rangle$  as the product of two factors: (a) the probability that  $N_1 > 0$  and (b) the conditioned expectation of  $\tilde{N}_1$ , to be denoted by  $\langle \langle \tilde{N}_1(L, \eta) \rangle \rangle$ , which is computed by considering only the stacks within which  $\tilde{N}_1$  does not vanish. To evaluate factor (a), it suffices to project our surface  $B(P) = 0$  onto the "floor" of the big cube. This projection has a well-defined positive area. Factor (a) is obtained by dividing this area by  $L^2$ ; it is non zero and has the same value for the central lines of all possible stacks. Finally, we show that factor (b) is proportional to  $(L/\eta)^{0.5}$ . This task can be reduced to proving that, within a time  $t$  after the beginning of a discrete random walk, the expected number

of its returns to the point of departure is proportional to  $t^{1/2}$ . This last fact is well-known; see Feller 1968 (p. 86, Theorem 2).

### 2.10. A conjecture

A stronger result is known for  $\tilde{N}_1$ , namely that  $\tilde{N}_1(L, \eta)/\langle \tilde{N}_1(L, \eta) \rangle$  is a universal random variable. The same result is doubtlessly true (but I did not attempt to prove it) of the ratio  $N(L, \eta)/\langle N(L, \eta) \rangle$ . If this conjecture were confirmed, one could show that the limit  $\lim_{\eta \rightarrow 0} N(L, \eta)/\log(L/\eta)$  would involve no randomness and could serve as an alternative definition of  $D$ . This definition is more like the mathematical theory of fractal dimensions and the definition used in my earlier applications, where  $D$  was defined as either  $D = \log N / \log(L/\eta)$  or as some limit of this expression for  $\eta \rightarrow 0$ . For example, when attempting to show that coastlines are best regarded as curves with a dimension  $D$  between 1 and 2, I argued (a) that a coastline is self-similar in the sense that one can, by selecting  $N-1$  points on any piece of it, subdivide it into subpieces reduced from the whole by a similarity of ratio  $r$  and (b) that, as  $r \rightarrow 0$ ,  $\log N / \log r^{-1}$  has a limit that serves to define  $D$ .

In a different application, in which I showed that certain error patterns are best regarded as a set with a dimension  $D$  below 1, I proved that the counterpart of  $N(L, \eta)/\langle N(L, \eta) \rangle$  is a universal random term.

## 3. GEOMETRY OF RANDOM SCALAR FIELDS WITH KOLMOGOROV VARIANCE AND WEIGHTED POISSON AND GAUSSIAN DISTRIBUTIONS; THESE ARE FRACTIONAL BROWNIAN FUNCTIONS OF A POINT

Now we consider the Gaussian field  $\tilde{B}(P)$ , with  $\langle [\tilde{B}(P') - \tilde{B}(P'')] \rangle = 0$  and the Kolmogorov variance  $\langle [\tilde{B}(P') - \tilde{B}(P'')]^2 \rangle = |\overline{P'P''}|^{2/3}$ . The approximations  $B(P)$  and  $\tilde{B}(P)$  are special cases, corresponding to  $H=1/2$  and  $H=1/3$  respectively, of the more general one-parameter family of Gaussian fields  $B_H(P)$  such that the variance

$$\langle [\tilde{B}(P') - \tilde{B}(P'')]^2 \rangle = |\overline{P'P''}|^{2H},$$

where  $H$  is a constant between 0 and 1. The case where  $H \neq 1/2$  and  $P$  is restricted to a line was alluded to by Kolmogorov 1940 and has been widely used since M & Van Ness 1968{H11} who coined for it the term

"fractional Brownian process." The case where the space of  $P$  is multi-dimensional was briefly alluded to by Yaglom 1957 and by Gangolli 1967 and studied in M 1975b{H17}.

**Fractional Poisson fields: sharp discontinuity.** Let us continue to assume everything previously said about Poisson fields, with the following exception: the definition of  $D_n F(P)$  is replaced by  $D_n \tilde{F}(P) - D_n \tilde{F}(O)$ , where  $D_n \tilde{F}(P)$  vanishes if  $\overline{OP} \cdot \overline{OH_n} = R_n$  and elsewhere is replaced by

$$D_n \tilde{F}(P) = 2^{-1} Q_n \operatorname{sgn} [\overline{OP} \cdot \overline{OH_n} - R_n] [\overline{OP} \cdot \overline{OH_n} - R_n]^{-1/6}.$$

If the exponent is 0 instead of  $-1/6$ , then  $D_n \tilde{F}(P)$  is again  $D_n F(P)$  plus an additive factor, which makes it easier to normalize  $\tilde{F}(O)$  to zero. The most striking facts about  $\tilde{F}(P)$  are that  $\tilde{F}(P) - \tilde{F}(P'')$  tends to infinity near each discontinuity plane and that it is affected by every one of an infinite number of close or distant discontinuity planes. By way of contrast,  $F(P)$  was only affected by the finite number of planes which intersect the segment  $\overline{PP''}$ . Thus, the elementary steps required for the variance to follow the  $2/3$  law are extremely global.

**Probability distribution in a scalar weighted probability field.** Again, as in Section 2, the distribution of  $F(P)$  tends to a Gaussian as  $|\overline{OP}| \rightarrow \infty$ .

**Continuity in fractional Brownian fields.** As before, the field  $\lambda^{-1/2} \lambda(P)$  is defined such that its variance is independent of  $\lambda$  and its limit  $\lambda \rightarrow \infty$  is a Gaussian field and hence identical to  $\tilde{B}(P)$ . One can prove that this limit is continuous (almost surely and almost everywhere). Recall that  $B(P)$  was also continuous; this property is less obvious here than it was for  $B(P)$ , because the jumps in  $\lambda^{-1/2} D_n F(P)$  tended to zero as  $\lambda \rightarrow \infty$ , while  $\lambda^{-1/2} D_n \tilde{F}(P)$  remains (for all  $\lambda$ ) grossly discontinuous. (Thus, the small steps in the limit are obtained as the product of 0 and  $\infty$ , rather than the product of 0 and 1.)

**Iso-surfaces.** In the fractional case, the Poisson iso-surfaces are less useful than in the Burgers case. A first difference in the iso-surface is that they are no longer made up of small pieces of a plane. Second, the fact that  $\tilde{F}(P)$  tends to infinity near one side of each plane of discontinuity means that each iso-surface is cut up into small pieces, each of them located within one of the bounded polyhedrons defined by the planes of discontinuity. However, these features cease to be drawbacks in simulations because  $\tilde{F}(P)$  is necessarily interpolated from its values computed on a discrete grid. Figure 2 shows several successive "slices" of the volume

enclosed by a sample fractional Brownian iso-surface. It was obtained by interpolating a sample fractional Poisson iso-surface  $\tilde{B}(P)=0$ , which, again, was constructed using a Gaussian distribution for the  $Q_n$ . The qualitative description given in the caption of Figure 1 also applies here, but the irregularity is accentuated even more.

*The fractal dimension of the iso-surface is equal to  $3 - 1/3$  and for the surface  $[x, y, z, B(x, y, z)]$  it is doubtlessly equal to  $4 - 1/3$ .* All the arguments concerning the fractal dimension proceed exactly as in Section 2 until the point where  $\langle\langle N_1(L, \eta) \rangle\rangle$  is shown to be proportional to  $(L/\eta)^{0.5}$ . The difference is that, for the linear cross-sections that are fractional Brownian scalar motions of exponent  $H$ , this factor equals  $(L/\eta)^{1-H}$ . For turbulence, we know that  $H = 1/3$ .

*A self-similar random field that is not Gaussian cannot be approximated by a Poisson field.* The increments of a field  $F(P)$  are called self-similar if one can rescale them to obtain a function  $A(|\overline{OP}|)[F(P) - F(O)]$  having a distribution independent of  $P$ . One can show that as a result,  $A(|\overline{OP}|)$  must be a power of  $|\overline{OP}|$ , and it follows that the degree of flatness (also the kurtosis) of  $F(P)$  must be independent of  $P$ . Furthermore, one can show that the only self-similar Gaussian fields are those of the above form  $B_H(P)$  and that the only weighted Poisson fields with a variance of the form  $|\overline{OP}|^{2H}$  are also those described above. Hence, we see that attempts to obtain a non-Gaussian self-similar field as the limit of weighted Poisson fields are doomed. In Section 5, the field  $F(P)$  will be replaced by a vector field, which can (and in turbulence must) be skew; therefore, the warning expressed by this last remark will extend to the impossibility of approximating skew fields using Poisson fields. This result means that the plane discontinuities used above are mere mathematical devices, devoid of physical meaning. This feature might have been suspected, given the profoundly nonlinear character of turbulence. The question then arises of whether or not the above results concerning the role and value of fractal dimensions continue to apply to non-Gaussian fields. The answer is not known, and it may well remain unknown until very specific details of the distribution of the field are determined.

#### 4. DEGREES OF LOCALITY IN SCALAR FIELDS

This section will be devoted to the study of local and global characteristics in Gaussian fields having either Burgers or Kolmogorov variance or more generally, the variance  $|\overline{P'P''}|^{2H}$  with  $0 < H < 1$  (called fractional if  $2H \neq 1$ ).



It is best to begin with a visual comparison of the figures in M 1975O, M 1975w{H19}. Both exhibit sample functions of  $B(x, y, 0)$  for  $H = 1/2$  and  $1/3$ . The latter case is "flatter," and its strong high-frequency detail overwhelms a weak low-frequency background.

**The field  $B(P)$  with Burgers variance.** All rectilinear cross-sections of  $B(P)$ , such as  $B(x, 0, 0)$ , are classical Brownian motions on a line, which are well-known to have the Markov property. If one knows  $B(0, 0, 0)$ , which we may set equal to zero, then all  $B(x, 0, 0)$  for  $x < 0$  are independent from all  $B(x, 0, 0)$ , for  $x > 0$ . Hence, the conditional distribution of  $B(x_0, 0, 0)$ , for a fixed  $x_0 > 0$ , is the same if one knows  $B(x, 0, 0)$  only for  $x = 0$  or if one also knows  $B(x, 0, 0)$  for any number of points  $x_n < 0 (n \geq 1)$ . Also, if one knows  $B(0, 0, 0)$  and  $B(x_0, 0, 0)$ , added information about the value of  $B(x, 0, 0)$  outside the interval  $[0, x_0]$  does not change the conditional distribution of  $B(x, 0, 0)$  within that interval. For example, let  $B(x, 0, 0)$  be conditioned by known values of  $B(0, 0, 0)$ , of  $B(x_0, 0, 0)$  and of  $B(x_k, 0, 0)$  for any number of points  $x_k$  inside  $(0, x_0)$ . In that case, the extrapolate obtained as the expected conditional value of  $B(x, 0, 0)$  is equal to  $B(0, 0, 0)$  for  $x < 0$ , and to  $B(x_0, 0, 0)$  for  $x > x_0$ . If it is conditioned by  $B(0, 0, 0)$ , by  $B(x_0, 0, 0)$  and by the values of  $B(x, 0, 0)$  for any number of points  $x_k$  outside  $(0, x_0)$ ,

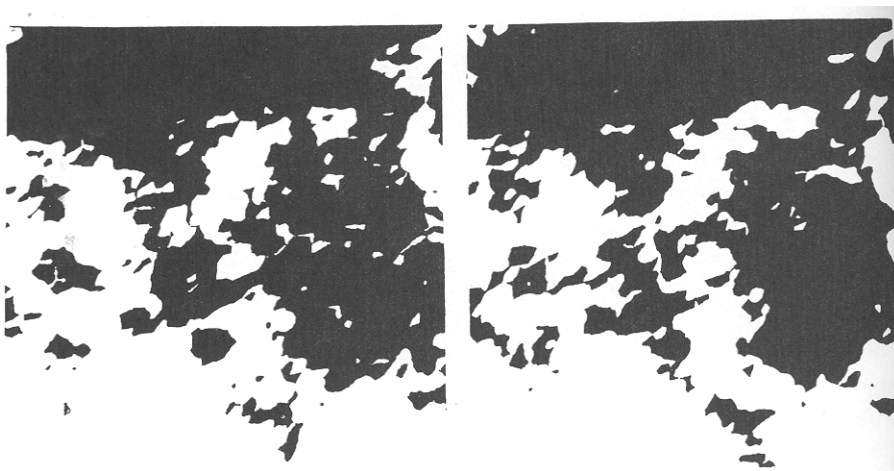


FIGURE C18-2. Two successive slices of a computer-generated approximation to the volume  $\tilde{B}(P) > 0$ , where  $\tilde{B}(P)$  is the Gaussian approximation to a Kolmogorov scalar field. Here, (contrary to Figure 1) the interpenetrating black and white regions are very much alike in their appearance. The resemblance between this graph and ink splotches (which almost caused it to be destroyed) enhances the feeling that it represents some genuine feature of the actual motion of fluids.

the interpolate is linear. This last feature expresses that the local behavior of  $B(x, 0, 0)$  in any bounded domain on the line is determined by its values on the domain's boundary plus additional random effects of local nature.

For the field  $B(P)$  in space, the situation is somewhat different. The local behavior of  $B(x, 0, 0)$  continues to be determined locally, but the meaning of the term "local" changes substantially. On the one hand, Lévy 1948 showed that, if  $B(x, y, 0)$  is known on the horizontal plane, its values above and below that plane are *not* independent; in fact they have a strong negative correlation. Hence, knowing the value  $B(0, 0, z)$  *does change* the distribution of the value  $B(0, 0, -z)$ . Similarly, if  $B(P)$  is known on a sphere including  $O$ , knowing the value  $B(0, 0, 0)$  *does change* the distribution of  $B(P)$  outside the sphere. On the other hand, McKean 1963 showed that, if  $B(P)$  is known on *two* non-intersecting spheres containing  $O$ , the distributions of  $B(P)$  at two points, one inside and the other outside both spheres, are indeed independent; this result is called a two-stage Markov property. Thus, it remains true that the distribution of  $B(P)$  within a small bounded domain is determined locally, but one must redefine this last term to imply a knowledge of  $B(P)$  on a double (not a single) boundary.

**The field  $\tilde{B}(P)$  with Kolmogorov variance.** Compared with the spectral density  $k^{-2}$  of the Burgers field  $B(P)$ , the spectral density  $k^{-5/3}$  of  $\tilde{B}(P)$  is richer in high-frequency harmonics and poorer in low-frequency harmonics, which indicates that it should be even more local, if anything. However, this issue deserves a more careful examination. We begin again with  $\tilde{B}(x, 0, 0)$  as an example of a rectilinear cross-section. It is the fractional Brownian random function of one parameter ("time"). It is highly non-Markovian, that is,  $\tilde{B}(0, 0, 0) = 0$  being known, the additional knowledge of any value  $\tilde{B}(x', 0, 0)$ , where  $x' < 0$ , will affect strongly the distribution of  $\tilde{B}(x_0', 0, 0)$ , especially when  $x_0' = -x'$ . *A fortiori*, the same is true of  $\tilde{B}(P)$  in space. However, curiously, this feature is fully compatible with an appropriately weakened concept of what is "local."

**The field  $B_H(P)$  for which the increments' variance is  $\overline{P'P''}^{2H}$ .** This last characteristic continues to hold true for all Gaussian fields  $B_H(P)$  such that  $\langle [B_H(P') - B_H(P'')]^2 \rangle = \overline{P'P''}^{2H}$ , with  $0 < H < 1/2$ . The overall effect of knowing  $B_H(O) = 0$  and  $B_H(P_0)$  with  $P_0 = (x_0', 0, 0)$ , can be assessed by examining the conditional expected value of  $B_H(P)$ . One finds

$$\langle [B_H(P) - 1/2B_H(P_0)] | B_H(P_0) \rangle = Q B_H(P_0)$$

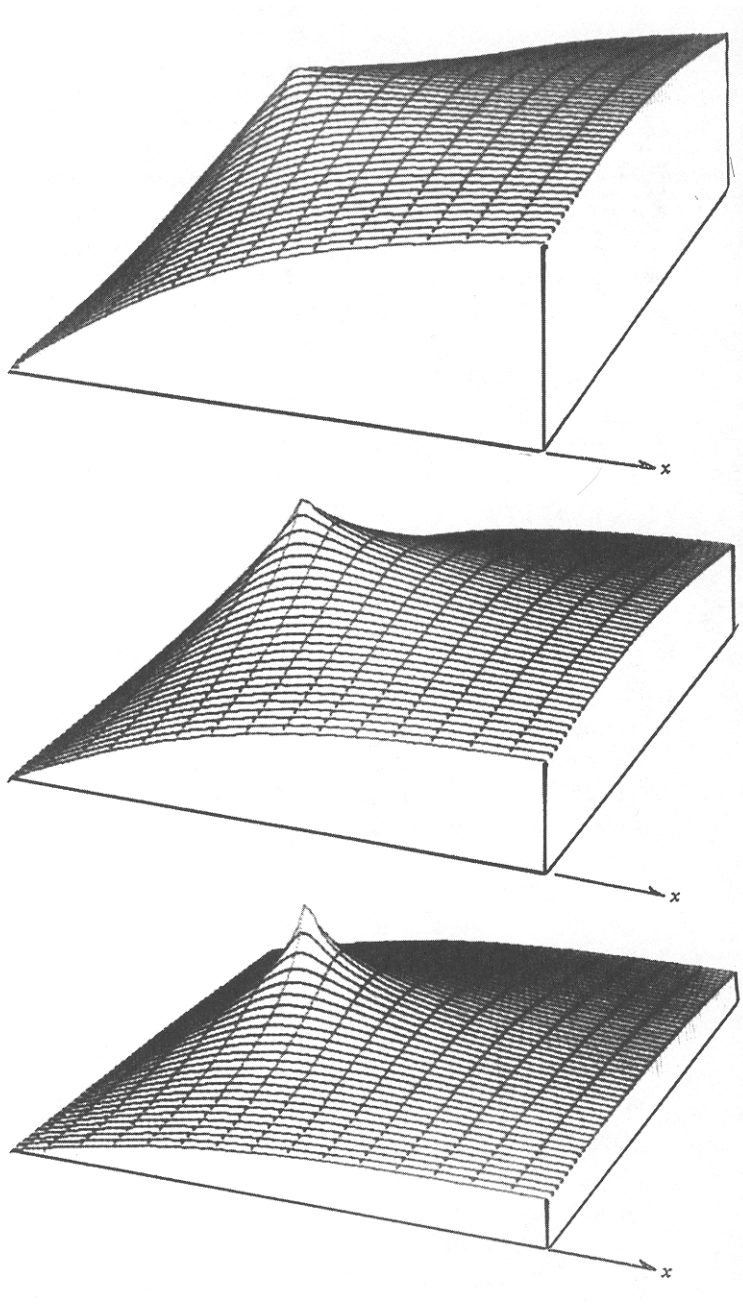


FIGURE C18-3. The function  $Q(x,y,0)$  for  $x > 1/2$ . The peak's abscissa is  $x=1$ . (a)  $H=1/2$ , (b)  $H=1/3$  and (c)  $H=1/6$ .

with

$$Q = \frac{1}{2} \left[ \left( \frac{\overline{OP}}{x_0} \right)^{2H} - \left( \frac{\overline{PP_0}}{x_0} \right)^{2H} \right].$$

To simplify, we shall henceforth set  $x_0 = 1$ . When  $P$  lies on the line from  $O$  to  $P_0$ ,  $Q$  reduces to

$$Q = 1/2[|x|^{2H} - |1-x|^{2H}].$$

We have already described the behavior of the function  $Q$  when  $H$  takes the Markov value  $1/2$  and  $P$  lies on the straight line joining  $O$  and  $P_0$ . Let us extend the examination to other values of  $H$  and  $P$ . For all  $H$ ,  $Q = 0$  along the plane  $x = 1/2$ ,  $Q > 0$  for  $x > 1/2$  and  $Q < 0$  for  $x < 1/2$ .

More specifically, let  $H = 1/2$ . The iso- $Q$ -surfaces are hyperboloids with rotational symmetry around the  $x$ -axis. Also, when  $x > 1$  and  $x^2 + y^2 + z^2 = r^2 \gg 1$ , one has  $Q \sim x/r$ , which means that, within a cone around the  $x$  axis,  $Q$  is close to its upper bound of unity. A perspective view of the surface  $Q(x, y, 0)$  is shown in Figure 3(a). Its behavior shows that, when  $|\overline{OP}| \gg |\overline{OP_0}|$  and when  $B(O)$  and  $B(P_0)$  are known, the conditioned distribution of  $B(P)$  depends strongly on the precise relative positions of  $P, O$  and  $P_0$ . Conversely, in some cases, such as when  $x \gg 1$  and  $y = z = 0$ ,  $B(P)$  affects the distribution of  $B(P_0)$  but not the distribution of  $B(O) - B(P_0)$ . In other cases, as when  $r \gg 1$ , and  $x$  is near zero,  $B(P)$  affects the distribution of  $1/2[B(P_0) + B(O)]$  but hardly that of  $B(O) - B(P_0)$ .

Now let  $H < 1/2$ . Two perspective views of the surface  $Q(x, y, 0)$  and a precise graph for  $y = z = 0$  are shown in Figures 3(b), 3(c) and 4. In the last figure, for  $x = 1/2$ ,  $Q = 1/2$  and has a slope equal to  $H \times 2^{1-2H}$  (for  $H = 1/3$  the slope is equal to 0.84); at the points  $x = 0$  and  $x = 1$ , it has cusps, but over most of  $(0, 1)$  it is not too far from being straight. When  $P$  is on the  $x$ -axis outside  $(0, 1)$ ,  $Q$  tends to zero. The same is true when going away from  $O$  along other directions, since it is readily seen that, when  $r^2 = x^2 + y^2 + z^2 \gg 1$ ,  $Q_H \sim (x/r)r^{2H-1}$ . Thus, for  $H \neq 1/2$  and  $r \gg 1$ , the conditioned distribution of  $B_H(P)$ , knowing  $B_H(O)$  and  $B_H(P_0)$ , depends primarily on  $1/2[B_H(O) + B_H(P_0)]$ ; knowledge of the precise relative positions of  $O, P$  and  $P_0$  leads only to a second-order correction. Conversely,  $B_H(P)$  mostly affects the local average  $1/2[B_H(O) + B_H(P_0)]$  and hardly affects the distribution of  $B_H(O) - B_H(P_0)$ .

In summary, neither  $B(P)$  nor  $B_H(P)$  is strictly local for  $H < 1/2$ . But from certain viewpoints, locality is more marked for  $B_H(P)$  than for  $B(P)$ . This is already true when  $H = 1/3$ . If  $H$  is below the Kolmogorov value  $1/3$ , this locality is accentuated more.

The more local behavior of  $Q$  near  $O$  and  $P_0$  is also worth further exploration, if only to confirm that it is indeed "local." This is a region where the expected behavior of  $B_H(P)$  is more important in comparison with the random component. We see that the local shape is likely to consist of a sharp pit located next to a sharp peak, where "sharp" means extending a distance that is a small multiple of  $x_0$ . This feature explains, in part, the presence of small pieces of "jetsam and flotsam" observed earlier in the paper.

## 5. GEOMETRY OF SOME RANDOM VECTOR FIELDS

We shall sketch the generalization of the results to vector fields with Burgers variance in Sections 2 and 3. They may assist in building intuition, but their counterpart for the case of Kolmogorov variance is likely to

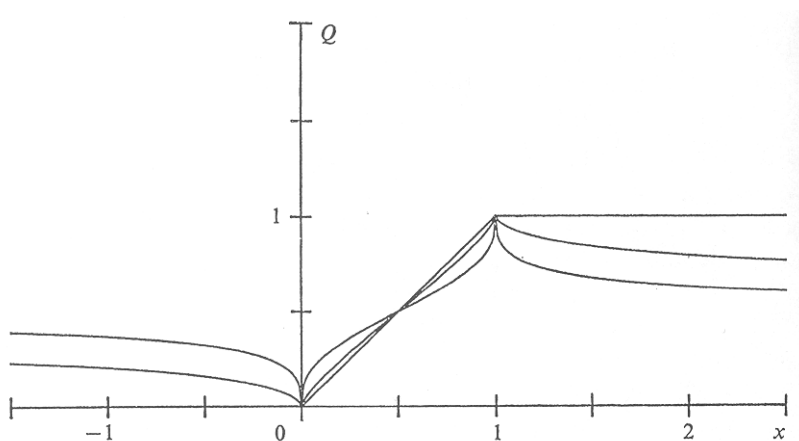


FIGURE C18-4. The function  $Q(x, 0, 0)$ , corresponding to  $P$  lying on the line joining  $O$  and  $P_0$ . To the right (or to the left) of  $x = 1/2$ ,  $Q$  is a monotone increasing (or decreasing) function of  $H$ . Its behavior is shown for  $H = 1/6, 1/3$  and  $1/2$ .

have limited use. The reason is that in turbulence skewness is essential but there is no natural way of building it into turbulence using the approach in this paper. For example, one can show that the probability distribution in a weighted Poisson field is such that, while  $\langle [F(P) - F(O)]^2 \rangle = |\overline{OP}|^{2H}$ ,  $\langle [F(P) - F(O)]^3 \rangle$  equals  $|\overline{OP}|^{3H-0.5}$  if  $H > 1/6$  and is roughly constant if  $H < 1/6$ . Hence, the skewness of  $F(P) - F(O)$  unavoidably tends to zero as  $|\overline{OP}|$  increases.

*Brownian vector fields.* A Brownian vector field (normalized, for the sake of convenience, to satisfy  $B(O)=0$ ) can be defined naturally as a vector  $B(P)$  such that its normal component and its two tangential components are independent Gaussian random variables of variance proportional to  $|\overline{OP}|$ . It is easy to see that the normal component is at most as large as either of the tangential ones; this follows from the Kármán-Howarth 1938 reduction of a correlation term to the functions that they call  $f(r, t)$  and  $g(r, t)$ .

*Poisson vector fields.* Similarly, one can generate a Poisson field such that its planar discontinuities have both normal and tangential components.

**Brownian limits of Poisson vector fields.** Given a sequence of Poisson fields  $F_\lambda(P)$ , the expression  $\lim_{\lambda \rightarrow \infty} F_\lambda(P)$  is a Brownian field  $B(P)$ . But it is a special Brownian field because the vector  $B(P) - B(O)$  is isotropic at every point. (In the familiar Kármán-Howarth notation, the functions  $f(x, t)$  and  $g(x, t)$  are identical.)

&&&&&&&&&& ANNOTATION &&&&&&&&&&

*An episode in the very early history of word processing on the computer.* This story and a related one are told in Section 4.6 of Chapter H8.